USP35 promotes cell proliferation and chemotherapeutic resistance through stabilizing FUCA1 in colorectal cancer

Pengju Zhang (✉ zhpj@sdu.edu.cn)
   School of Basic Medical Sciences, Cheeloo College of Medicine

Yi Xiao

Xiaoyu Jiang

Tianshu Miao

Hanlin Lu

Wenqing Wang

Lijuan Ma

Yinghui Zhao
   City Of Hope National Medical Center

Chunyan Liu

Yun Qiao

Article

Abstract

Ubiquitin-specific-processing proteases 35 (USP35) is an under-characterized deubiquitinase and its role in colorectal cancer (CRC) remains unclear. Here, we focus on delineating the impact of USP35 on CRC cell proliferation and chemo-resistance, as well as the possible regulatory mechanism. By examining the genomic database and clinical samples, we found that USP35 was overexpressed in CRC. Further functional studies showed that enhanced USP35 expression promoted CRC cell proliferation and resistance to oxaliplatin (OXA) and 5-fluorouracil (5-FU), whereas USP35 depletion impeded cell proliferation and sensitized cells to OXA and 5-FU treatments. Then, to explore the possible mechanism underlying USP35-triggered cellular responses, we performed co-immunoprecipitation (co-IP) followed by mass spectrometry (MS) analysis and identified α-L-fucosidase 1 (FUCA1) as a direct deubiquitiation target of USP35. Importantly, we demonstrated that FUCA1 was an essential mediator for USP35-induced cell proliferation and chemo-resistance in vitro and in vivo. Finally, we observed that nucleotide excision repair (NER) components (e.g., XPC, XPA, ERCC1) were up-regulated by USP35-FUCA1 axis, indicating a potential mechanism for USP35-FUCA1-mediated platinum resistance in CRC. Together, our results for the first time explored the role and important mechanism of USP35 in CRC cell proliferation and chemotherapeutic response, providing a rationale for USP35-FUCA1-targeted therapy in CRC.

Highlights

- USP35 promotes cell proliferation and resistance to oxaliplatin and 5-fluorouracil in CRC.
- USP35 deubiquitinates and stabilizes FUCA1.
- FUCA1 mediates the function of USP35 on CRC proliferation and chemo-resistance.
- USP35-FUCA1 axis contributes to oxaliplatin resistance via up-regulating nucleotide excision repair.

1. Introduction

Colorectal cancer (CRC) is a prevalent and lethal malignancy worldwide [12]. It is the third most commonly diagnosed cancer and the third leading cause of cancer-related mortality in men and women in the United States [33]. Although CRC is a detectable and curable disease if diagnosed at an early stage, nearly two-third of the patients is diagnosed at advanced stages with a stark decrease in 5-year survival rate [1, 12, 33]. For the local CRC, endoscopic and surgical removals are the mainstay treatments, whereas for the regional and metastatic cases, surgery as well as systemic treatment, including adjuvant chemotherapy, targeted therapy, immunotherapy, radiotherapy, etc. are required [1]. Of note, identifying critical cancer targets for targeted therapy has been of tremendous interest in the biomedical field over the past two decades, aiming to increase the specificity in cancer treatment and overcome drug resistance of the traditional regimens [50]. In the case of CRC, new options of targeted therapy have been unceasingly revealed, bringing great therapeutic avenue for the cancer patients [41]. Therefore, unraveling novel targets in CRC will offer new opportunities in improving treatments for the CRC patients.

Ubiquitination is a common post-translational modification that by affecting protein stability, interaction, localization, and activity, regulates fundamental biological process, including cell division, fate specification, migration, etc. [29, 44]. Aberrant protein ubiquitination due to altered expression or activity of ubiquitin-activating enzyme (E1), ubiquitin-conjugating enzyme (E2), ubiquitin ligase (E3), deubiquitinase (DUB), and proteosome, contributes to cancer development [13, 29]. Drugs targeting ubiquitin-proteasome system (UPS) components have achieved substantial progress in cancer treatment, with several proteasome inhibitors approved by the Food and Drug Administration (FDA) and many other inhibitors actively tested in pre-clinical studies [13, 25]. DUBs function to catalyze the removal of ubiquitin (Ub) moieties from targeted proteins, and accumulating evidence has suggested that DUBs are attractive therapeutic targets owing to the well categorized catalytic domains [3, 9–11, 20, 21]. Up to now, there are roughly 100 identified human DUBs, and the characteristics of many DUBs are still unknown [9]. Here, we aim to understand the role of one of the under-characterized DUBs, ubiquitin-specific-processing proteases 35 (USP35), in this study.

USP35 is a member of the cysteine proteases C19 family [28]. Recent works have suggested that USP35 is a promising cancer target due to its role in tumor growth and chemo-resistance by regulating the stability of important players in tumor development and cell death [6, 23, 36, 40, 48]. For example, USP35 promotes tumorigenesis in estrogen receptor (ER) positive breast cancer by stabilizing and activating estrogen receptor α (Erα) to increases Erα transcriptional activity [6]. USP35 resists cancer cell apoptosis through mitigating endoplasmic reticulum stress (ERS) by deubiquitinating RRBP1 or stabilizing anti-apoptotic factor BIRC3 [23, 40]. USP35 also reduces ferroptosis by enhancing ferroportin-mediated iron export [36]. Moreover, USP35 suppresses the induction of type I interferons by interfering with STING-TBK1-IRF3 pathway [48]. Despite the potential role of USP35 in tumorigenesis and drug resistance, there is still a knowledge gap concerning the role of USP35 in CRC. Hence, we focus on investigating how USP35 affects carcinogenesis and drug resistance in CRC.

Altered glycosylation is a common feature in cancer and of great clinical significance in cancer screening, diagnosis, targeted therapy, and prognosis [37]. In our journey to find the possible mechanism, through which USP35 exerts its role in CRC, we identified α-L-fucosidase 1 (FUCA1) as a potential target. FUCA1 is an enzyme that hydrolyzes terminal fucose residues from glycolipids or glycoproteins [4, 26], and its function in cancers remains obscure and controversial. While a few studies suggest that FUCA1, as a transcriptional target of p53, restrains tumor growth, attenuates cell motility, triggers cell death, and sensitizes cancer cells to chemotherapy [5, 17, 39], two other studies lead to quite opposite conclusions [8, 42]. Therefore, we performed a series of functional studies under the regulation of USP35-FUCA1 axis, aiming to better understand the role of FUCA1 in cancers.

In the present study, we first demonstrated that USP35 promoted CRC cell proliferation and resistance to the drugs (oxaliplatin and 5-fluorouracil) routinely used in the CRC clinic. Then, we performed co-immunoprecipitation (co-IP) followed by mass spectrometry (MS) analysis, and identified FUCA1 as a potential target of USP35. We further confirmed that FUCA1 was deubiquitinated and stabilized by

USP35. Additionally, we showed that the impact of USP35 on CRC cell growth and chemo-resistance was mediated by FUCA1 *in vitro* and *in vivo*. Finally, we suggested that USP35-FUCA1 axis up-regulated nucleotide excision repair (NER) components (e.g., XPC, XPA, ERCC1), which could be a potential mechanism for platinum resistance in CRC. Overall, this study indicates that USP35 contributes to tumorigenesis and confers chemo-resistance in CRC by deubiquitinating FUCA1, unraveling a novel molecular target for CRC treatment.

2. Materials And Methods

2.1 Cell culture and transfection

HEK293T and CRC cell lines (DLD-1, LoVo, HT29 and HCT116) were purchased from the Cell Bank of the Chinese Academy of Science (Shanghai, China) and cultured following the instructions. Cells were resuscitated every three months and tested negative for mycoplasma contamination.

Polyethylenimine (PEI, polysciences, Inc.) was used for transfection. psPAX2 and pMD2.G (GeneChem Co.) were used for lentiviral packaging. RFect (Changzhou Bio-generating) was used as transfection reagent. The transfection was conducted following the manufacturer's instructions.

2.2 Expression constructs and RNA interference

Human wild-type (WT) USP35 vectors pCMV-3X-HA-USP35/HA-USP35 and pCMV-3X-Myc-USP35/Myc-USP35, and the catalytically inactive USP35 mutant pCMV-3X-HA-USP35 C450A/USP35 C450A were previously constructed by our laboratory [22, 40]. Human FUCA1 vector pcDNA3.1-Flag-FUCA1 was purchased from Fenghui Biotechnology Co. USP35 cDNA was cloned into the pLVX-IRES-Puro vector (Addgene) for lentivirus production. The specific shRNAs was cloned into the pLKO.1-TRC vector (GenePharma) and the targeting sequences are: shUSP35-1: 5'-GCTGAGTTGGGCTCTTCTAGA-3'; shUSP35-2: 5'-GCGTCTGACTTCAGACATTG-3'; shFUCA1-1: 5'-CGCAGAGTTTGCTTGGACTAT-3'; shFUCA1-2: 5'-GCAACTATCTTCTGAACATTG-3'; shFUCA1-3: 5'-GGAAATGGCTGAGCATCAATG-3'; shFUCA1-4: 5'-GGTCCACAGATCCAGATAATT-3'. The non-effective scrambled shRNA targeting sequence is 5'-GTTCTCCGAACGTGTCACGT-3'.

2.3 Western blotting, co-immunoprecipitation, and mass spec. analysis

Western blotting (WB) and co-immunoprecipitation (co-IP) were performed as previously described [40].

The Flag-tagged USP35 expression plasmid or the empty vector were transfected into the HCT116 cell line. The USP35-associated proteins were co-immunoprecipitated with anti-Flag antibody. The proteins were then separated by SDS-PAGE and stained with Fast Silver Stain Kit (Beyotime Biotechnology). The band of interest was cut for mass spec. analysis according to previously mentioned protocol [40].

2.4 Antibodies and reagents

The antibodies used in our experiments were listed in Table S1. 5-fluorouracil (5-FU, APExBIO) and oxaliplatin (OXA, GlpBio) were stocked at a concentration of 3 mg/mL and 10 mg/mL in water, respectively. MG132 and cycloheximide (Calbiochem) were stocked and used as previously described [40].

2.5 Cell viability, apoptosis, and immunofluorescence

The cell viability was measured by clonogenic and Cell Counting Kit-8 (CCK-8, APExBIO) assays. For clonogenic assay, 2000 cells were seeded in the 6-well plates. 7 days after the seeding, cells were washed with PBS, fixed with 4% paraformaldehyde in PBS, and stained with Giemsa staining solution (Solarbio Life Science). For CCK-8 assay, 2000 cells were seeded in the 96-well plates for 48 hours to examine the cell viability. Or else, 2000 cells were seeded in the 96-well plates for 24 hours, and then the indicated drugs were added into the cells for 48-hour treatments at different concentrations or for different time duration to examine the drug toxicity. The cell viability was examined by CCK-8 according to manufacturer's instruction.

The cell apoptosis was measured by Annexin V/Propidium Iodide (PI) staining followed by flow cytometry analysis or terminal dUTP nick-end labeling (TUNEL) assay as previously described [40].

The immunofluorescence (IF) staining and confocal microscopy were performed following the similar procedures as previously done [40].

2.6 Xenograft mouse model

5-week-old male athymic nude mice were purchased from HFK Bioscience Company. 5×10^5 HT29 cells were subcutaneously inoculated into the flanks of the mouse (5 mice per group). A week after the inoculation, water, OXA (10 mg/kg in water), or OXA (5 mg/kg in water) plus 5-FU (50 mg/kg in water), was intraperitoneally injected in the mice weekly, and tumor size was measured every three days. The tumor volume (V) was calculated by the formula: $V = 0.5 \times length \times width^2$. Mice were euthanized by cervical dislocation at the end of the experiment. The animals were bred in pathogen-free conditions and experimental procedures were approved by the Institutional Animal Care and Use Committee of Shandong University.

2.7 Immunohistochemistry and scoring

30 human CRC tissues along with their adjacent noncancerous tissues were obtained from the tumor tissue bank from the Affiliated Hospital of Qingdao University (Qingdao, China). Informed consent was obtained from the patients for this study. The immunohistochemistry (IHC) staining and the blind scoring were performed as previously described by two pathologists [23, 47].

2.8 Statistical analysis

GraphPad Prism 8 software (La Jolla, CA, USA) was used for statistical analyses. The quantified data were presented as the mean ± SD of at least three independent experiments. Different groups were compared using unpaired, two-tailed, Student's t-test. Spearman's correlation analysis was used for

analyzing the correlation between the expression of USP35 and FUCA1 in the CRC samples. *P* < 0.05 was considered statistically significant.

2.9 Data availability

The USP35 gene expression data in human CRC tissues and the non-cancerous tissues were derived from TCGA and GEO (GSE37182, GSE21815, and GSE71187) database. The USP35 expression levels correlated with tumor stage as well as the recurrence rate in CRC patients receiving postoperative chemotherapy were derived from TCGA database. All the data supporting the findings of this study are available from the corresponding author on reasonable request.

3. Results

3.1 USP35 is overexpressed in CRC patients

To explore the role of USP35 in CRC, we first checked its expression in CRC patients. According to the TCGA and GEO (GSE37182, GSE21815, and GSE71187) databases, USP35 mRNA levels were increased in CRC patients (Fig. 1A and 1B, Fig. S1). We further examined USP35 protein expression in our CRC patient samples through immunohistochemistry (IHC) staining and western blotting (WB). Consistently, the USP35 expression was higher by approximately two folds in the cancerous tissues compared to the non-cancerous tissues (Fig. 1C and 1D). Moreover, the TCGA data also suggested that high expression of USP35 was associated with increased cancer stages in CRC patients and higher recurrence rate in CRC patients receiving postoperative chemotherapy (Fig. 1E and 1F). These data suggest that USP35 is elevated in CRC, and overexpression of USP35 is associated with CRC progression and recurrence, potentiating USP35 as a cancer target in CRC.

3.2 USP35 promotes CRC cell proliferation and chemo-resistance

To understand the impact of USP35 on CRC cell proliferation, we overexpressed USP35 in LoVo and HT29 cells, and depleted USP35 in DLD-1 and HCT116 cells (Fig. 2A, Fig. S2A). The cell proliferation was monitored by Cell Counting Kit-8 (CCK-8) and clonogenic assays. We found that augmented expression of USP35 promoted cell viability as well as clonogenic activity in LoVo and HT29 cells (Fig. 2B and 2C). USP35 deficiency, however, dampened the proliferation in DLD-1 and HCT116 cell lines, as indicated in Fig. S2B and S2C. These results show that USP35 is required for CRC cell proliferation.

Since USP35 expression was comparatively higher in CRC recurrent cases (Fig. 1F), we next investigated whether USP35 contributed to chemo-resistance in CRC cell lines. Oxaliplatin (OXA) and 5-fluorouracil (5-FU) are classical drugs in the CRC chemotherapy regimens, either as single or combination therapy [1]. We therefore examined whether USP35 affected CRC cell response to OXA, 5-FU, or the combined treatment of OXA and 5-FU. We first tested whether increased USP35 expression conferred resistance to OXA, 5-FU, or combination of OXA and 5-FU in HT29 cell lines. We treated the HT29 cells using single or double

agents with different concentration or at different time points, and examined the cell viability through CCK-8 assay. We found that USP35 overexpression rendered HT29 cells more resistant to the cytotoxic agents, either on the condition of single or combined treatments (Fig. 2D and 2E). We then tested whether USP35 depletion sensitized cells to the chemotherapies using the similar methods, and found that USP35 ablation enhanced cytotoxic effects of those drugs on the DLD-1 cells (Fig. S2D and S2E). The impact of USP35 on cell apoptosis in response to OXA, 5-FU, or combination of OXA and 5-FU was further detected by Annexin V/Propidium Iodide (PI) staining flow cytometry analysis and terminal dUTP nick-end labeling (TUNEL) assay. Strikingly, USP35 overexpression markedly reduced cytotoxic agents-induced cell apoptosis (Fig. 2F and 2G), while USP35 knockdown led to increased drug-induced cell apoptosis (Fig. S3C and S3D). The quantified data of apoptotic cells were presented in Fig. S3A-D.

3.3 USP35 deubiquitinates and stabilizes FUCA1

To investigate the possible mechanism for USP35-mediated cell proliferation and drug resistance, we transfected Flag-tagged USP35 expression plasmid into the HCT116 cell line, immunoprecipitated the USP35-associated proteins with anti-Flag antibody, separated the proteins by SDS-PAGE, and analyzed the immunoprecipitated proteins by mass spectrometry (Fig. 3A). Mass spectrometry identified seven candidates (PRMT5, PPM1B, FUCA1, DNAJA1, IGF2BP1, DDX5, XRCC6) which may be associated with USP35 (Fig. S4A). Among these potential targets of USP35, we would like to specifically focus on α-L-fucosidase 1 (FUCA1) in our current study (Fig. 3B, Fig. S4B and S4C), considering the strong relevance of altered glycosylation in cancer development and therapeutics [37].

To validate our screened results, we first examined whether the physical interaction existed between USP35 and FUCA1. Co-immunoprecipitation (co-IP) assay was used for this purpose. HEK293T cells were transfected with Myc-tagged USP35 and/or Flag-tagged FUCA1, the USP35- or FUCA1-associated proteins were immunoprecipitated with anti-Myc or anti-Flag antibodies, and the lysates were subject to western blotting analysis. As illustrated in Fig. 3C and 3D, USP35 interacted with FUCA1 in a reciprocal fashion. The interaction between endogenous USP35 and FUCA1 was also detected in LoVo and DLD-1 cells (Fig. 3E and 3F). Moreover, we checked the localization of USP35 and FUCA1 in the CRC cell lines using immunofluorescence (IF) staining followed by confocal microscopy. We found that there was a similar expression pattern for USP35 and FUCA1, with enhanced expression in the nuclei and modest expression in the cytosols (Fig. 3G and 3H).

Considering USP35 is a deubiquitinase, we then investigated whether FUCA1 was deubiquitinated by USP35. We transiently transfected HEK293T cells with Flag-tagged FUCA1, HA-tagged wild-type USP35 (USP35 WT), or HA-tagged catalytically inactive USP35 (USP35 C450A) [27] plasmids, immunoprecipitated FUCA1 associated proteins with anti-Flag antibody, and probed for ubiquitin (Ub) by western blotting. The proteasome inhibitor MG132 was used to enrich the USP35 and FUCA1 proteins in the cells. We found that only the catalytically active USP35 (USP35 WT), not the USP35 mutant (USP35 C450A), deubiquitinated FUCA1 (Fig. 4A). This result indicated that USP35 removed ubiquitins from FUCA1 and its enzymatic activity was required for this function. In addition, we silenced the USP35-overexpressed cells

with different dose of shRNAs, and found that the ubiquitination of FUCA1 was increased with USP35 depletion in a dose dependent manner (Fig. 4B). This result further confirmed that FUCA1 was a deubiquitination target of USP35.

Given the most widespread outcome of protein ubiquitination is the alteration of protein stability [2], we next investigated whether USP35 affected FUCA1 stability. Cycloheximide (CHX) chase assay was used to measure the stability of FUCA1 with different USP35 expression levels. We found that overexpression of wild-type USP35 (USP35 WT), not the catalytically inactive mutant USP35 (USP35 C450A), prevented FUCA1 from degradation in LoVo cells, whereas knockdown of USP35 accelerated FUCA1 degradation in DLD-1 cells (Fig. 4C and 4D). Resultantly, enhanced USP35 expression increased FUCA1 at protein levels in CRC cells and HEK293T in a dose dependent manner (Fig. S5A and S5B), while dampened USP35 expression clearly decreased the protein levels of FUCA1 in DLD-1 and HCT116 cells (Fig. S5C). As expected, USP35 overexpression or silencing didn't affect the mRNA levels of FUCA1 (Fig. S5D and S5E). Since proteasome is required in the ubiquitin-proteasome pathway for protein degradation, we further tested how altered expression of USP35 would affect the levels of FUCA1 in the presence of MG132. As a result, forced expression of USP35 in LoVo and HT29 cells failed to "wax" FUCA1, and depletion of USP35 in DLD-1 and HCT116 cells failed to "wane" FUCA1 as it usually did with addition of MG132 (Fig. 4E and 4F), indicating USP35 protected FUCA1 from proteasome-mediated degradation. Overall, these results demonstrate that USP35 deubiquitinates FUCA1 and increases FUCA1 stability by preventing ubiquitin-proteasome pathway-mediated degradation of FUCA1.

3.4 FUCA1 mediates the effect of USP35 on cell proliferation and chemo-resistance *in vitro*

Considering the previously reported role of FUCA1 in cancer growth and chemo-resistance [5, 8, 17, 39, 42], we here investigated whether the influence of USP35 on cell proliferation and drug resistance was mediated or partially mediated by FUCA1 in our study.

We first knocked down FUCA1 in USP35-overexpressed LoVo and HT29 cells, using FUCA1-specific shRNA-4 with higher knockdown efficiency (Fig. S6A and S6B). As shown in Fig. 5A, FUCA1 expression was reduced to approximately the basal levels by FUCA1-specific shRNA-4 in the USP35-overexpressed LoVo and HT29 cells. Interestingly, FUCA1 ablation almost completely reversed proliferation-promoted effect of USP35 on LoVo and HT29 cells, as indicated by clonogenic and CCK-8 assays (Fig. 5B and 5C). Then, we stably overexpressed FUCA1 in USP35-depleted DLD-1 and HCT116 cell lines to restore FUCA1 expression to the near-basal levels (Fig. S7A). Consequently, augmented FUCA1 substantially ameliorated the growth-inhibitory effect of USP35 deficiency on these cells (Fig. S7B and S7C).

Next, we investigated whether USP35-triggered OXA and 5-FU resistance was associated with FUCA1 expression. Cells were subject to OXA, 5-FU, or combination treatments using similar conditions as in Fig. 3, and the drug toxicity was measured by CCK-8 assay. As a result, FUCA1 depletion fully re-sensitized the USP35-overexpressed HT29 cells to different chemotherapeutic treatments (Fig. 5D, Fig.

S7E). However, boosted FUCA1 expression largely de-sensitized USP35-depleted cells to the similar treatments in DLD-1 cells (Fig. S7D, Fig. S8A). Moreover, drug-induced apoptosis in these cells was illustrated by Annexin V/PI staining flow cytometry analysis and TUNEL assay. We found that depleting FUCA1 in USP35-overexpressed cells led to an increase of apoptotic cells to a rate as the control (EV + shNC) cells (Fig. 5E and 5F, Fig. S8B and S8C), whilst re-expressing FUCA1 in USP35-deficient cell decreased apoptotic cell population to the similar level as control (Scramble + Vector) cells in response to cytotoxic insults (Fig. S8D and S8E). Together, these data suggest that FUCA1 is an essential player that mediates USP35-associated cell proliferation and OXA/5-FU resistance in CRC cells.

3.5 FUCA1 mediates the impact of USP35 on tumor growth and chemo-resistance *in vivo*

To explore the role of USP35-FUCA1 axis *in vivo*, we subcutaneously inoculated the control (EV + shNC), USP35-overexpressed (USP35 + shNC), and USP35 overexpressed FUCA1-depleted (USP35 + shFUCA1-4) HT29 cells in the athymic nude mice, intraperitoneally injected water (H_2O), single drug (OXA as a representative), or combined drugs (OXA + 5-FU) weekly into the mice, and routinely monitored the tumor growth. We observed that USP35 overexpression markedly promoted tumor growth and drug resistance, but depleting FUCA1 in USP35-overexpressed cells reversed the tumor growth to the basal levels, and re-sensitized the tumors to the chemo-treatments, as indicated by representative images, tumor weight and growth curve (Fig. 6A-C).

Next, we examined the USP35-FUCA1 axis in the human CRC tissues. A total of 30 human CRC samples were included for IHC staining and analysis. As shown in the representative images, USP35 and FUCA1 shared the similar expression pattern (Fig. 6D). For example, in some samples, USP35 and FUCA1 were both intensely expressed in the CRC epithelium and lightly stained in the CRC stroma (Fig. 6D, sample 1). In the samples with low USP35 expression, FUCA1 expression was usually barely detectable (Fig. 6D, sample 2). According to the assessment by the pathologists, among 25 USP35-highly-expressed CRC samples, 20 samples expressed elevated FUCA1, and among 5 USP35-lowly-expressed CRC samples, 4 samples exhibited reduced FUCA1 expression (Fig. 6E). The strong correlation between USP35 and FUCA1 expression levels in the CRC tissues was further verified by Spearman's correlation analysis ($p < 0.001$ and $r = 0.665$, Fig. 6F). We also examined the expression of USP35 and FUCA1 in human CRC tissues as well as adjacent normal tissues by western blotting, and found that FUCA1 expression was largely in accordant with USP35 expression (Fig. 6G). The quantified western blotting data and correlation analysis were shown in Fig. S9A and S9B. Therefore, these results suggest that USP35 expression correlates well with FUCA1 expression in CRC patient samples, and USP35-FUCA1 axis contributes to CRC tumor growth and chemo-resistance *in vivo*.

3.6 USP35-FUCA1 axis up-regulates nucleotide excision repair in CRC.

Two studies demonstrated that USP35 deficiency sensitized cancer cells to cisplatin (the first platinum anti-cancer drug) treatment via de-stabilizing anti-apoptotic factor BIRC3 or activating cGAS-STING-TBK1-

mediated expression of type I interferons [23, 48]. However, another study showed that FUCA1, as a direct transcriptional target of p53, was required for cisplatin-induced cell apoptosis [5]. Given that the latter study was in discrepant with our findings, which might be due to the different experimental settings, we here investigated the possible mechanism of USP35-FUCA1-mediated oxaliplatin (the third-generation platinum drug) resistance in CRC.

The Pt-based chemotherapies work by introducing DNA-platinum adducts, which is mainly corrected by nucleotide excision repair (NER) [18, 45]. Increased NER proficiency is one of the reasons accounting for on-target resistance of Pt-based therapy [18, 30]. We therefore examined the expression levels of some major components (e.g., XPC, XPA, ERCC1) of the NER system [31]. We found that in USP35-overexpressed LoVo and HT29 cells, the expression levels of XPC, XPA and ERCC1 were markedly increased (Fig. S10A and S10B, Fig. S11A and S11B). Accordingly, the XPC, XPA and ERCC1 levels were decreased by USP35 knockdown in a dose-dependent manner in DLD-1 and HCT116 cells (Fig. S10C and S10D, Fig. S11C and S11D). Moreover, ablating FUCA1 in HT29 cells dramatically reduced the expression of XPC, XPA and ERCC1, whereas enhancement of FUCA1 largely restored the level of these NER components (Fig. S10E and S10F, Fig. S11E and S11F). Hence, our current results indicate that USP35-FUCA1 axis up-regulates NER in CRC cells, which may be a possible mechanism for USP35-FUCA1-mediated oxaliplatin resistance in CRC.

4. Discussion

Despite the limited studies exploring the functions of USP35 in cancers, recent evidence has suggested that USP35 is a potential cancer target that regulates tumorigenesis, cell death, and cancer immunology [6, 22, 23, 36, 40, 48]. Interestingly, out of these six studies, three studies investigated the role of USP35 in cell death, including RRBP1-mediated ERS-triggered apoptosis [40], BIRC3-mediated cisplatin-triggered apoptosis [23], and ferroportin-mediated iron overload-triggered ferroptosis [36]. Our study has further demonstrated that USP35 is a cell death-related deubiquitinase that prevents oxaliplatin- and 5-fluorouracil-induced apoptosis in CRC. Overall, the mechanism of cell death is highly diversified, which can be categorized into programmed apoptosis, programmed non-apoptotic cell death (e.g., ferroptosis, pyroptosis, mitoptosis, etc.), and necrosis [43]. While the current studies give us a glimpse of how USP35 participates in cell death, there is still a lot to explore to determine whether USP35 is indeed a master regulator that can affect cell death in multiple ways. Resisting cell death is one of the hallmarks of cancer and targeting cell death pathway (e.g., Bcl-2) has achieved encouraging results in clinics [19, 34]. Additionally, many apoptosis-targeted therapies are being actively tested in clinical trials [7]. Given the druggable nature of DUBs [3, 21], this study provides pre-clinical evidence that USP35 is an apoptotic-associated DUB that may be targeted and applied in the CRC therapeutics.

Apart from the cell death-associated role of USP35, two other aspects of USP35 seem to be very intriguing to us as well — its participation in mitosis and cancer immunology. A study led by Park et al. showed that USP35 was required for mitotic progression, and Aurora B was a deubiquitination target of

USP35 [27]. The mitotic role of USP35 places it in an appealing spot for targeting, considering that mitosis is a promising anti-cancer target [15, 38]. Their study also raises a question whether targeting USP35 will modulate Taxol response. Taxol is a clinically used microtubule-targeting agent (MTA) that exerts the cytotoxic effect by inducing chromosome mis-segregation [46]. It is possible that USP35 inhibition may synergize with Taxol to induce apoptosis or cell arrest, based on the result that USP35 deficiency itself already leads to multiple mitotic errors, and this outcome could be further exacerbated by Taxol treatment [27]. As for the involvement of USP35 in cancer immunology, two studies indicated that USP35 overexpression was associated with immune-suppressive tumor microenvironment (TME), especially the decrease in CD8$^+$ T cell infiltration [48, 49]. In the study of Zhang et al., the authors further illustrated that USP35 repressed cGAS-STING-interferon signaling, which could be the reason for reduced CD8$^+$ T cell infiltration in ovarian cancer [48]. Although immuno-oncology is an old concept, it really ushered into a new era in cancer care with series of new drugs under development and investigation [14, 16]. Compared with traditional cancer treatments (e.g., chemotherapy and radiotherapy), immunotherapy has considerable advantages, such as high accuracy, thoroughness, less toxicity, etc. [35]. However, immunotherapy is also complicated, due to the largely differed response rate, which can be affected by tissue specificities, TME, and individual difference [16, 35]. Thus, understanding the molecular drivers for immune-suppressive TME will improve individualized treatment in cancer immunotherapy. The previous studies have connected USP35 to immune microenvironment to some levels, and future studies may shed more light on whether and how targeting USP35 will activate the immune system against cancers in different models.

In this study, we have found that FUCA1 mediates the function of USP35 on cell proliferation and chemo-resistance in CRC. This finding contradicts the result of a previous study claiming FUCA1 is required for cisplatin-induced cell apoptosis [5]. We believe the discrepancy in these findings may be due to the different cancer type, genetic background, or experimental settings. In searching for the possible mechanism of how USP35-FUCA1 axis contributes to oxaliplatin resistance in CRC, we examined the expression of the main DNA repair pathway for platinum-induced DNA damage response (DDR) — the nucleotide excision repair (NER). We found that NER components (e.g., XPC, XPA and ERCC1) was up-regulated by the USP35-FUCA1 axis and we considered it an underlying mechanism for USP35-FUCA1 axis-mediated oxaliplatin resistance in CRC. Nevertheless, whether USP35-FUCA1 axis promotes the expression of NER components at transcriptional levels, post-transcriptional modifications, translational levels, or post-translational modifications, warrants further investigation. Despite the fact that targeted therapy and immunotherapy have considerably advanced in the past few years, platinum (Pt) compounds still remain one of the most frequently used anti-neoplastic drugs in the clinic [30]. Pt compounds are often used in combination with other chemotherapeutic agents to overcome drug resistance and reduce toxicity in clinical settings [45]. Additionally, novel combinations of Pt-based therapies that mediate immune checkpoint response, DNA damage repair system, reactive Pt accumulation, synergistic apoptosis, etc., are gaining increased interest over the years, and are being actively tested in pre-clinical studies [30, 45]. This study offers a novel target as well as a perspective for Pt-based combination therapy.

5-fluorouracil is an anti-metabolic drug that inhibits thymidylate synthase (TS) activity and triggers DNA or RNA damage, and is commonly used for the treatments of many solid tumors [24]. Like all other conventional anti-cancer drugs, the clinical application of 5-FU is limited by the development of chemo-resistance [32]. The current known mechanisms of 5-FU resistance include altered metabolic enzymes, presence of cancer stem cells (CSCs) or emergence of CSCs-like properties, angiogenesis, increased DNA damage repair (e.g., base excision repair [BER], mismatch repair [MMR], and homologous recombination [HR]) [32]. Accordingly, several strategies have been proposed to overcome 5-fluorouracil resistance, such as combination therapy, improved drug delivery, use of resistance reversal agents, and inhibition of DNA damage repair [32]. Although our study has demonstrated that USP35-FUCA1 axis confers resistance to 5-FU in CRC, we didn't go further to explore the underlying mechanism. This area of study acquires a thorough investigation in the future considering the diverse mechanisms of 5-FU resistance.

In summary, this study has elucidated the role of USP35 in CRC cell proliferation and drug resistance. We have also demonstrated that FUCA1 is an important mediator for USP35 functions in CRC. Given the enzymatic activity of USP35 and FUCA1, we provide an outlook that targeting USP35-FUCA1 axis could be a plausible strategy for restricting tumor growth and chemo-resistance in CRC. The role of USP35 in CRC will be further investigated in different animal models. Moreover, USP35 will be pharmacologically targeted to examine the druggability, as well as the biological significance of USP35 in CRC.

Declarations

Conflict of interests

The authors declare no conflict of interests.

Author contributions

P.Z., Y.Q. and Y.X. designed the study and wrote the manuscript. P.Z. supervised the overall project. X.J. and Y. X. performed most of the cellular function and molecular mechanism assays, including cell proliferation and apoptosis experiments, quantitative real time PCR, immunofluorescence staining and western blotting. X.J., L.M. and T.M. performed nude mice xenograft model experiments. C.L. assisted in immunohistochemistry experiments. T.M. and Y.Z. performed bioinformatic analysis. W.W. and H.L. assisted in data analysis. X.J. finalized the figures. All authors approved the manuscript prior to submission.

References

1. Ahmed M (2020). Colon Cancer: A Clinician's Perspective in 2019. Gastroenterology research **13**: 1–10.

2. Amerik AY, Hochstrasser M (2004). Mechanism and function of deubiquitinating enzymes. Biochimica et Biophysica Acta (BBA) - Molecular Cell Research **1695**: 189–207.

3. Antao AM, Tyagi A, Kim KS, Ramakrishna S (2020). Advances in Deubiquitinating Enzyme Inhibition and Applications in Cancer Therapeutics. *Cancers* **12**.

4. Asfaw B, Schindler D, Ledvinová J, Cerný B, Smíd F, Conzelmann E (1998). Degradation of blood group A glycolipid A-6-2 by normal and mutant human skin fibroblasts. Journal of lipid research **39**: 1768–1780.

5. Baudot AD, Crighton D, O'Prey J, Somers J, Sierra Gonzalez P, Ryan KM (2016). p53 directly regulates the glycosidase FUCA1 to promote chemotherapy-induced cell death. Cell cycle (Georgetown, Tex) **15**: 2299–2308.

6. Cao J, Wu D, Wu G, Wang Y, Ren T, Wang Y *et al* (2021). USP35, regulated by estrogen and AKT, promotes breast tumorigenesis by stabilizing and enhancing transcriptional activity of estrogen receptor α. Cell Death Dis **12**: 619.

7. Carneiro BA, El-Deiry WS (2020). Targeting apoptosis in cancer therapy. Nat Rev Clin Oncol **17**: 395–417.

8. Cheng TC, Tu SH, Chen LC, Chen MY, Chen WY, Lin YK *et al* (2015). Down-regulation of α-L-fucosidase 1 expression confers inferior survival for triple-negative breast cancer patients by modulating the glycosylation status of the tumor cell surface. Oncotarget **6**: 21283–21300.

9. Clague MJ, Urbé S, Komander D (2019). Publisher Correction: Breaking the chains: deubiquitylating enzyme specificity begets function. Nature Reviews Molecular Cell Biology **20**: 321–321.

10. D'Arcy P, Wang X, Linder S (2015). Deubiquitinase inhibition as a cancer therapeutic strategy. Pharmacology & therapeutics **147**: 32–54.

11. De Cesare V, Carbajo Lopez D, Mabbitt PD, Fletcher AJ, Soetens M, Antico O *et al* (2021). Deubiquitinating enzyme amino acid profiling reveals a class of ubiquitin esterases. Proceedings of the National Academy of Sciences of the United States of America **118**.

12. Dekker E, Tanis PJ, Vleugels JLA, Kasi PM, Wallace MB (2019). Colorectal cancer. The Lancet **394**: 1467–1480.

13. Deng L, Meng T, Chen L, Wei W, Wang P (2020). The role of ubiquitination in tumorigenesis and targeted drug discovery. Signal Transduction and Targeted Therapy **5**: 11.

14. Dobosz P, Dzieciątkowski T (2019). The Intriguing History of Cancer Immunotherapy. Front Immunol **10**: 2965–2965.

15. Dominguez-Brauer C, Thu KL, Mason JM, Blaser H, Bray MR, Mak TW (2015). Targeting Mitosis in Cancer: Emerging Strategies. Molecular cell **60**: 524–536.

16. Esfahani K, Roudaia L, Buhlaiga N, Del Rincon SV, Papneja N, Miller WH, Jr. (2020). A review of cancer immunotherapy: from the past, to the present, to the future. Current oncology (Toronto, Ont)

27: S87-s97.

17. Ezawa I, Sawai Y, Kawase T, Okabe A, Tsutsumi S, Ichikawa H *et al* (2016). Novel p53 target gene FUCA1 encodes a fucosidase and regulates growth and survival of cancer cells. Cancer science **107**: 734–745.

18. Galluzzi L, Senovilla L, Vitale I, Michels J, Martins I, Kepp O *et al* (2012). Molecular mechanisms of cisplatin resistance. Oncogene **31**: 1869–1883.

19. Hanahan D (2022). Hallmarks of Cancer: New Dimensions. Cancer discovery **12**: 31–46.

20. Lai KP, Chen J, Tse WKF (2020). Role of Deubiquitinases in Human Cancers: Potential Targeted Therapy. International journal of molecular sciences **21**.

21. Lim KH, Baek KH (2013). Deubiquitinating enzymes as therapeutic targets in cancer. Current pharmaceutical design **19**: 4039–4052.

22. Liu C, Wang L, Chen W, Zhao S, Yin C, Lin Y *et al* (2015). USP35 activated by miR let-7a inhibits cell proliferation and NF-κB activation through stabilization of ABIN-2. Oncotarget **6**: 27891–27906.

23. Liu C, Chen Z, Ding X, Qiao Y, Li B (2022). Ubiquitin-specific protease 35 (USP35) mediates cisplatin-induced apoptosis by stabilizing BIRC3 in non-small cell lung cancer. Laboratory investigation; a journal of technical methods and pathology **102**: 524–533.

24. Longley DB, Harkin DP, Johnston PG (2003). 5-Fluorouracil: mechanisms of action and clinical strategies. Nature Reviews Cancer **3**: 330–338.

25. Morrow JK, Lin HK, Sun SC, Zhang S (2015). Targeting ubiquitination for cancer therapies. Future medicinal chemistry **7**: 2333–2350.

26. Occhiodoro T, Beckmann KR, Morris CP, Hopwood JJ (1989). Human α-L-fucosidase: Complete coding sequence form cDNA clones. Biochemical and biophysical research communications **164**: 439–445.

27. Park J, Kwon M-S, Kim EE, Lee H, Song EJ (2018). USP35 regulates mitotic progression by modulating the stability of Aurora B. Nature communications **9**: 688.

28. Quesada V, Díaz-Perales A, Gutiérrez-Fernández A, Garabaya C, Cal S, López-Otín C (2004). Cloning and enzymatic analysis of 22 novel human ubiquitin-specific proteases. Biochemical and biophysical research communications **314**: 54–62.

29. Rape M (2018). Ubiquitylation at the crossroads of development and disease. Nature Reviews Molecular Cell Biology **19**: 59–70.

30. Rottenberg S, Disler C, Perego P (2021). The rediscovery of platinum-based cancer therapy. Nature Reviews Cancer **21**: 37–50.

31. Schärer OD (2013). Nucleotide excision repair in eukaryotes. Cold Spring Harbor perspectives in biology **5**: a012609.

32. Sethy C, Kundu CN (2021). 5-Fluorouracil (5-FU) resistance and the new strategy to enhance the sensitivity against cancer: Implication of DNA repair inhibition. Biomedicine & Pharmacotherapy **137**: 111285.

33. Siegel RL, Miller KD, Fuchs HE, Jemal A (2022). Cancer statistics, 2022. CA: A Cancer Journal for Clinicians **72**: 7–33.

34. Strasser A, Vaux DL (2020). Cell Death in the Origin and Treatment of Cancer. Molecular cell **78**: 1045–1054.

35. Tan S, Li D, Zhu X (2020). Cancer immunotherapy: Pros, cons and beyond. Biomedicine & pharmacotherapy = Biomedecine & pharmacotherapie **124**: 109821.

36. Tang Z, Jiang W, Mao M, Zhao J, Chen J, Cheng N (2021). Deubiquitinase USP35 modulates ferroptosis in lung cancer via targeting ferroportin. Clinical and translational medicine **11**: e390.

37. Thomas D, Rathinavel AK, Radhakrishnan P (2021). Altered glycosylation in cancer: A promising target for biomarkers and therapeutics. Biochimica et biophysica acta Reviews on cancer **1875**: 188464.

38. Tischer J, Gergely F (2018). Anti-mitotic therapies in cancer. Journal of Cell Biology **218**: 10–11.

39. Vecchio G, Parascandolo A, Allocca C, Ugolini C, Basolo F, Moracci M *et al* (2017). Human a-L-fucosidase-1 attenuates the invasive properties of thyroid cancer. Oncotarget **8**: 27075–27092.

40. Wang W, Wang M, Xiao Y, Wang Y, Ma L, Guo L *et al* (2021). USP35 mitigates endoplasmic-reticulum-stress-induced apoptosis by stabilizing RRBP1 in non-small cell lung cancer. Molecular oncology.

41. Xie Y-H, Chen Y-X, Fang J-Y (2020). Comprehensive review of targeted therapy for colorectal cancer. Signal Transduction and Targeted Therapy **5**: 22.

42. Xu L, Li Z, Song S, Chen Q, Mo L, Wang C *et al* (2020). Downregulation of α-l-fucosidase 1 suppresses glioma progression by enhancing autophagy and inhibiting macrophage infiltration. Cancer science **111**: 2284–2296.

43. Multiple cell death modalities and their key features (Review).

44. Yau R, Rape M (2016). The increasing complexity of the ubiquitin code. Nature cell biology **18**: 579–586.

45. Yu C, Wang Z, Sun Z, Zhang L, Zhang W, Xu Y *et al* (2020). Platinum-Based Combination Therapy: Molecular Rationale, Current Clinical Uses, and Future Perspectives. Journal of Medicinal Chemistry **63**: 13397–13412.

46. Zasadil LM, Andersen KA, Yeum D, Rocque GB, Wilke LG, Tevaarwerk AJ *et al* (2014). Cytotoxicity of paclitaxel in breast cancer is due to chromosome missegregation on multipolar spindles. Science translational medicine **6**: 229ra243-229ra243.

47. Zhan P, Zhao S, Yan H, Yin C, Xiao Y, Wang Y *et al* (2017). alpha-enolase promotes tumorigenesis and metastasis via regulating AMPK/mTOR pathway in colorectal cancer. Molecular carcinogenesis **56**: 1427–1437.

48. Zhang J, Chen Y, Chen X, Zhang W, Zhao L, Weng L *et al* (2021). Deubiquitinase USP35 restrains STING-mediated interferon signaling in ovarian cancer. Cell death and differentiation **28**: 139–155.

49. Zhang Q, Liu YJ, Li JP, Zeng SH, Shen H, Han M *et al* (2022). USP35 is a Potential Immunosuppressive Factor in Skin Cutaneous Melanoma. Journal of inflammation research **15**:

3065–3082.

50. Zhong L, Li Y, Xiong L, Wang W, Wu M, Yuan T *et al* (2021). Small molecules in targeted cancer therapy: advances, challenges, and future perspectives. Signal Transduction and Targeted Therapy **6**: 201.
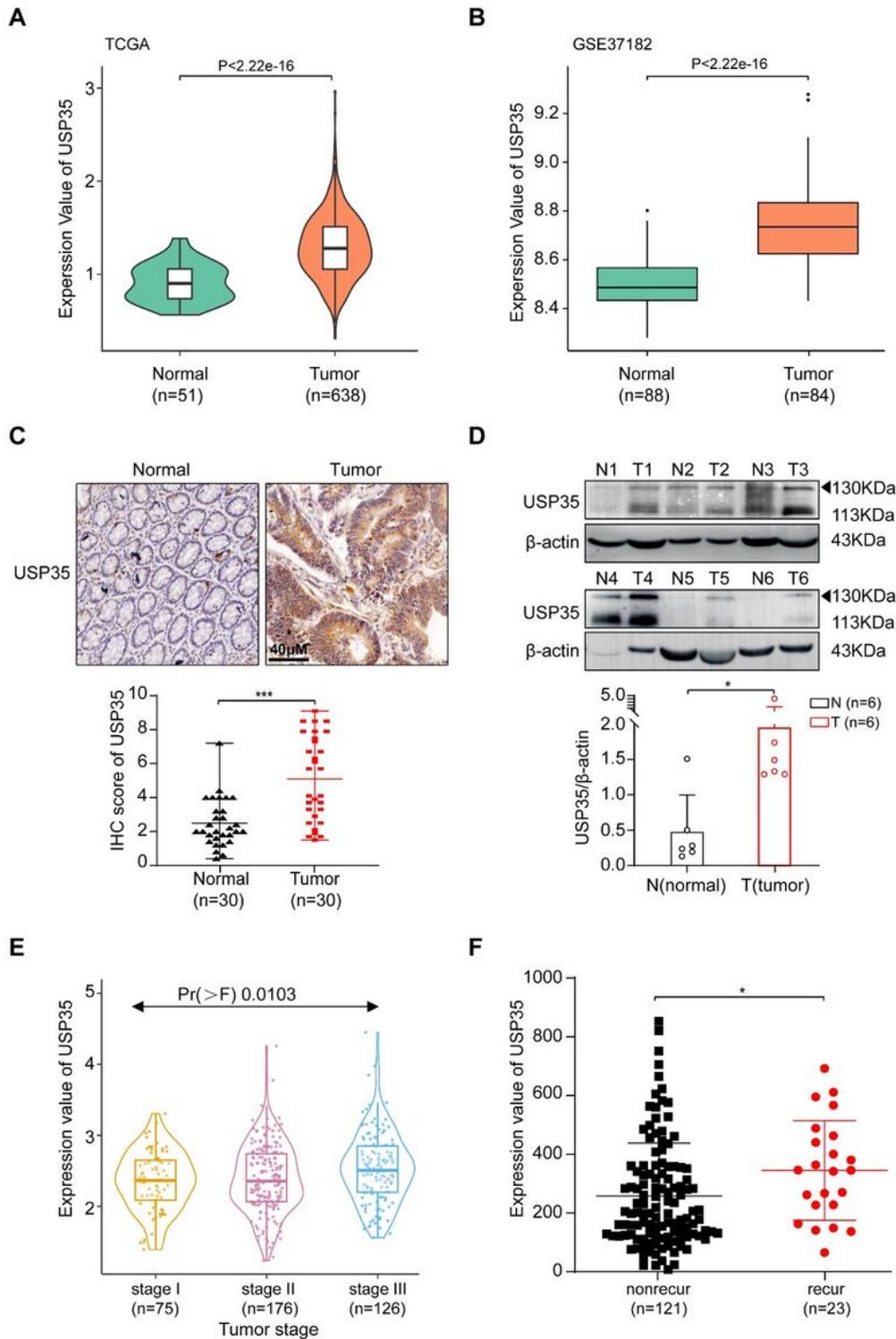
Figures

Figure 1

USP35 is overexpressed in CRC patients. (A, B) USP35 mRNA levels were higher in CRC patients according to the TCGA (A) and GEO (GSE37182) databases (B). (C) The representative immunohistochemistry stainings of USP35 in CRC tissues and adjacent tissues (n = 30). Quantitative analysis was shown in the graphs. (D) The expression levels of USP35 in CRC tissues and adjacent tissues were detected by western blotting (n = 8). Quantitative analysis was shown in the graphs. (E) High expression of USP35 was associated with increased cancer stages in CRC patients based on TCGA database. (F) The expression of USP35 was higher in the patients with recurrent (recur) CRC compared the patients with nonrecurrent (nonrecur) CRC after receiving chemotherapy. The data were extracted from the TCGA database. All data were presented by mean ± SD. *: $p < 0.05$, ***: $p < 0.001$ based on the Student's *t*-test.
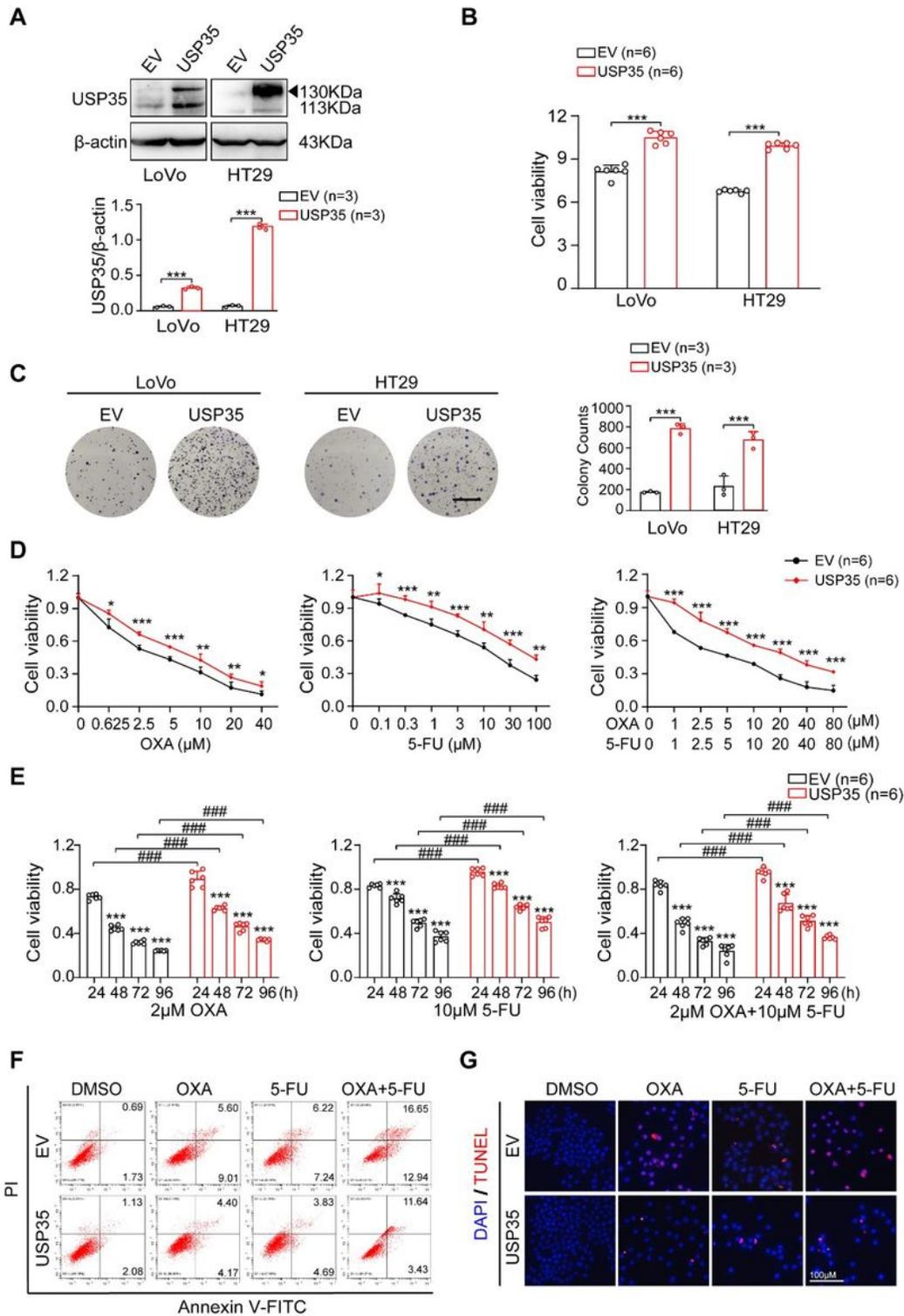
Figure 2

USP35 promotes CRC cell proliferation and chemo-resistance. (A) Establishment of USP35-overexpressed LoVo and HT29 cell lines. Quantitative analyses were shown in the graphs. (B) The cell viability of USP35-overexpressed LoVo and HT29 cells. Cells were implanted in 96-well plates for 48 hours (n = 6) and the cell viability was assessed using CCK8 assay. (C) Representative images of clonogenic assay (n = 3). USP35 overexpression promoted cell proliferation. Quantitative analyses were shown in the graphs.

The scale bars in represented 50 μm. (D) The USP35-overexpressed HT29 cells and the control cells were treated with different concentrations of oxaliplatin (OXA), 5-fluorouracil (5-FU), or combination of OXA and 5-FU for 48 hours (n = 6). The cell viability was assessed using CCK8 assay. (E) The USP35-overexpressed HT29 cells and the control cells were treated with OXA (10 μM), 5-FU (10 μM), or combination of OXA (10 μM) and 5-FU (10 μM) for 24, 48, 72, or 96 hours (n = 6). The cell viability was assessed using CCK8 assay. (F, G) The USP35-overexpressed HT29 cells and the control cells were treated with DMSO, OXA (10 μM), 5-FU (10 μM) or combination of OXA (10 μM) and 5-FU (10 μM) for 48 hours (n = 3). Representative images indicated the apoptotic cells detected by flow cytometry analysis (F) and TUNEL staining (G). Quantitative analyses were shown in the graphs. Data were presented as mean ± SD. *: $p<0.05$, **: $p<0.01$, ***: $p<0.001$, [#]: $p < 0.05$, [##]: $p < 0.01$, [###]: $p < 0.001$ based on the Student's t-test.
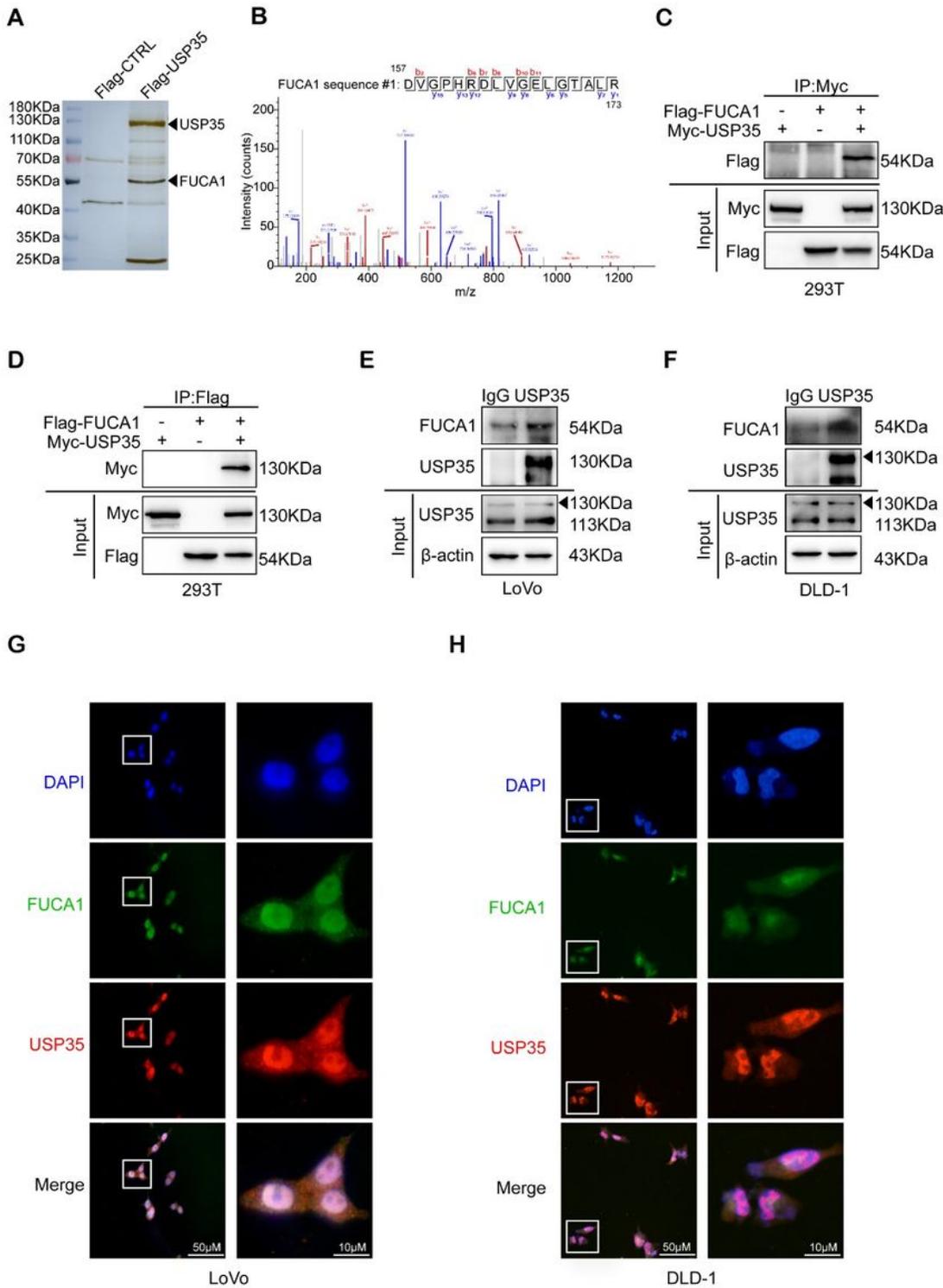
Figure 3

USP35 interacts with FUCA1. (A) Silver staining of the SDS-PAGE gel containing anti-Flag antibody immunoprecipitated proteins in Flag-USP35-overexpressed HCT116 cells and the control cells. (B) Representative map of mass spectrometry peaks of FUCA1 interacting with Flag-USP35.. (C, D) Exogenous interaction between USP35 and FUCA1. HEK293T cells were co-transfected with Flag-FUCA1 and/or Myc-USP35 plasmids. Cell lysates were immunoprecipitated with indicated antibodies, followed

by immunoblotting with anti-Flag antibody (C) or anti-Myc antibody (D). (E, F) Endogenous interaction between USP35 and FUCA1. Cell lysates from LoVo (E) and DLD-1 (D) were immunoprecipitated with anti-USP35 antibody or IgG antibody, followed by immunoblotting with anti-FUCA1 antibody. (G, H) Immunofluorescence staining and confocal microscopy showing USP35 and FUCA1 localization in LoVo (G) and DLD-1 (H) cells. Merged images indicated the overlapped area of USP35 and FUCA1 localization. The results were the representative of three independent experiments.
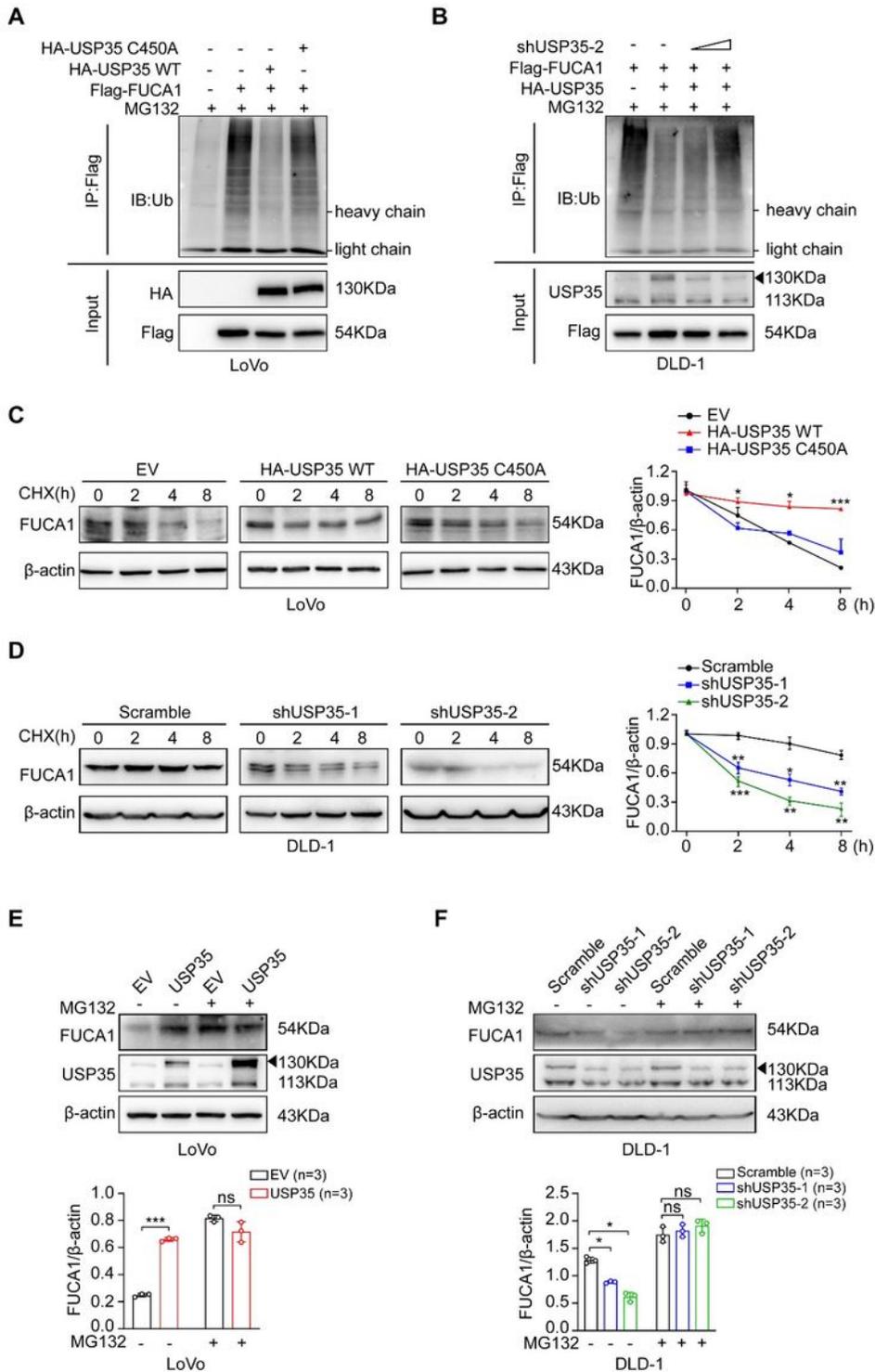
Figure 4

USP35 deubiquitinates and stabilizes FUCA1. (A, B) USP35 deubiquitinates FUCA1. (A) LoVo cells were transfected with Flag-FUCA1 alone or along with HA-tagged wild type USP35 (HA-USP35 WT) or the catalytically inactive USP35 (HA-USP35 C450A). Cell lysates were immunoprecipitated with anti-Flag antibody, followed by immunoblotting with anti-Ub antibody. MG132 was used to enrich the USP35 and FUCA1 proteins in the cells. (B) DLD-1 cells were transfected with Flag-FUCA1 alone or along with HA-USP35 WT and/or shUSP35-2 (0, 2 μg, or 4 μg). Cell lysates were immunoprecipitated with anti-Flag antibody, followed by immunoblotting with anti-Ub antibody. (C, D) USP35 increases the stability of FUCA1. LoVo cells expressing empty vector, HA-USP35 WT, or HA-USP35 C450A (C), and DLD-1 cells expressing USP35 specific scramble RNA, shUSP35-1, or shUSP35-2 (D) were treated with 50 μg/ml cycloheximide (CHX) for indicated time points. Then, the expression of FUCA1 was detected by western blotting. Quantitative analyses of CHX chase data were shown in the graphs. (E, F) USP35-mediated stabilization of FUCA1 is dependent on ubiquitin-proteasome system. USP35-overexpressed LoVo cells (USP35) and the control cells (EV) (E), and USP35-depleted DLD-1 cells (shUSP35-1 and shUSP35-2) and the control cells (Scramble) (F) were treated with or without 10 μM MG132 for 6 hours. The expression of FUCA1 was detected by western blotting. Quantitative analyses were shown in the graphs. Data were presented by mean ± SD of three independent experiments. ns: not significant. *: $p<0.05$, **: $p<0.01$, ***: $p<0.001$ based on the Student t-test.
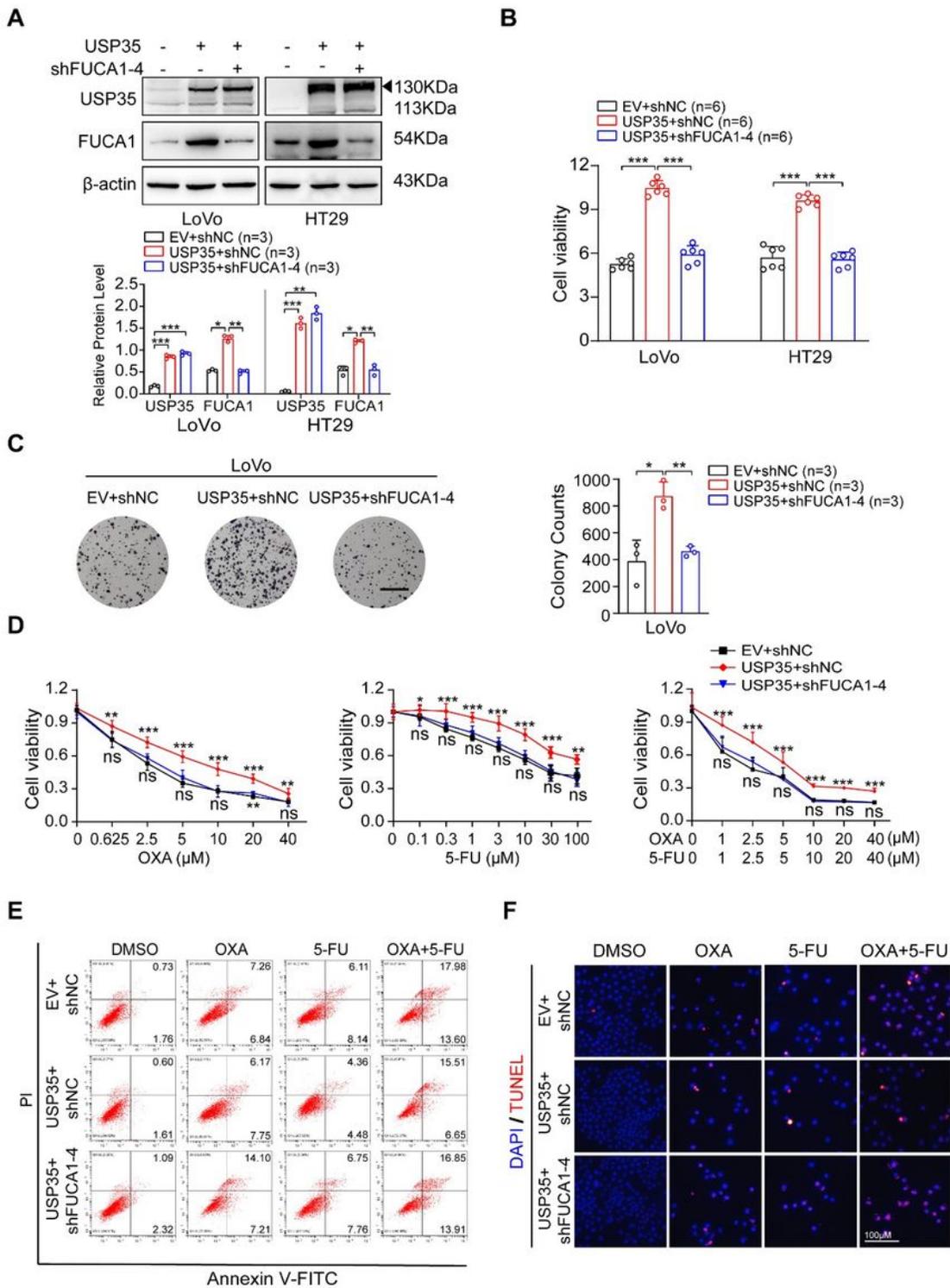
Figure 5

FUCA1 mediates the effect of USP35 on cell proliferation and chemo-resistance *in vitro*. (A) FUCA1-specific shRNA (shFUCA1-4) or control shRNA was introduced into the USP35-overexpressed HT29 and LoVo cells. The expression of FUCA1 and USP35 was detected by western blotting. Quantitative analysis was shown in the graphs. (B, C) CCK8 assay (B) and clonogenic assay (C) were used to detect the effect of FUCA1 depletion on USP35-induced cell proliferation. The scale bars in Fig. C represented 50 μM. (D)

FUCA1 specific shRNA (shFUCA1-4) or control shRNA was introduced into the USP35-overexpressed HT29 cells. The cells were treated with different concentrations of OXA, 5-FU, or combination of OXA and 5-FU for 48 hours (n = 6). The cell viability was assessed using CCK8 assay. (E, F) FUCA1-specific shRNA (shFUCA1-4) or control shRNA was introduced into the USP35-overexpressed HT29 cells. The cells were treated with DMSO, OXA (10 μM), 5-FU (10 μM) or combination of OXA (10 μM) and 5-FU (10 μM) for 48 hours (n = 3). Representative images indicated the apoptotic cells detected by flow cytometry analysis (E) and TUNEL staining (F). Data were presented as mean ± SD. ns: not significant. *: $p < 0.05$, **: $p < 0.01$, ***: $p < 0.001$ based on the Student's t-test.
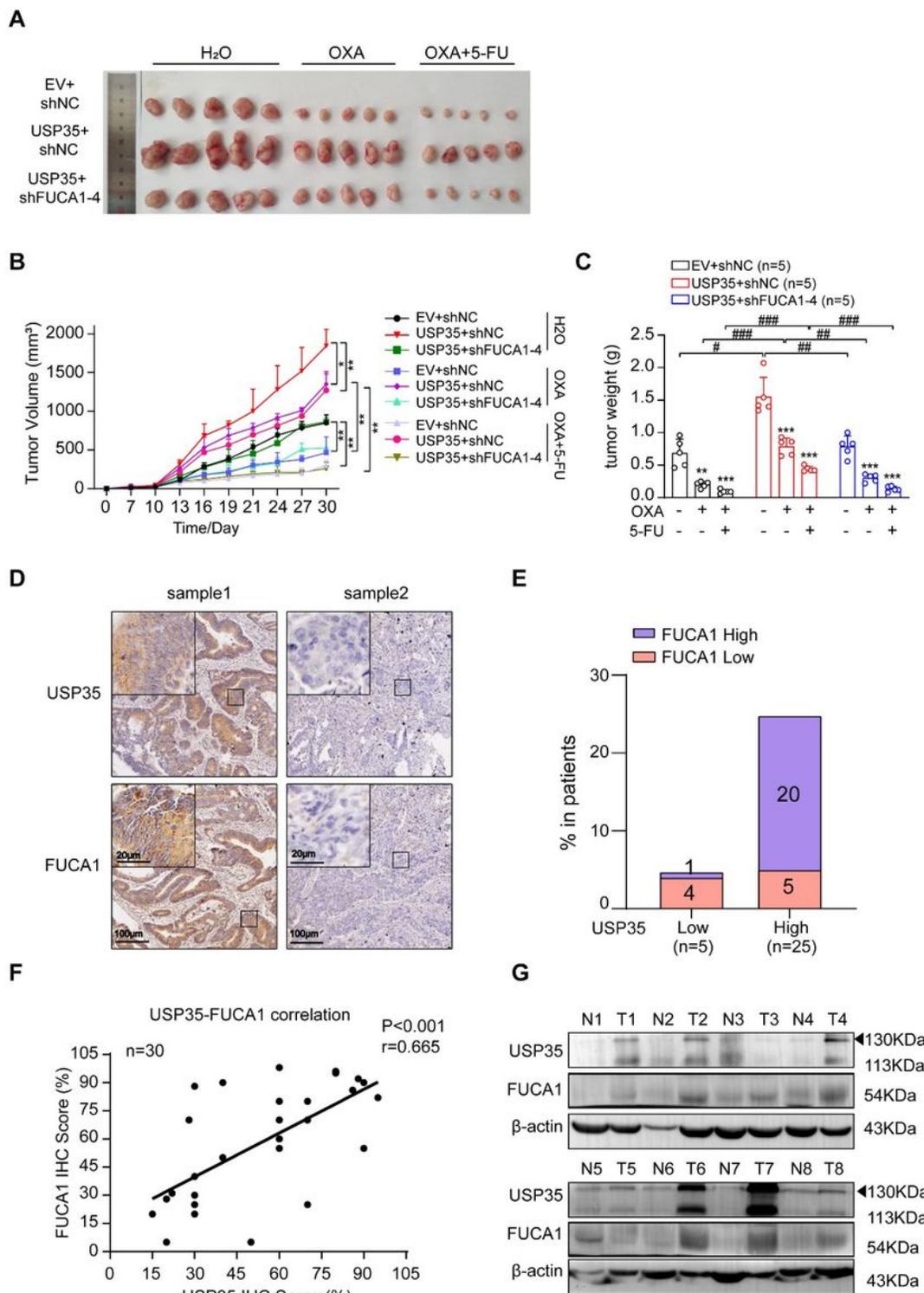
Figure 6

FUCA1 mediates the impact of USP35 on tumor growth and drug resistance *in vivo* (A) Tumor growth curve of HT29 cells with or without altered expression of USP35 or FUCA1. Cells were subcutaneously injected into the nude mice (n = 5). A week after the inoculation, water, OXA (10 mg/kg), or OXA (5 mg/kg) plus 5-FU (50 mg/kg), was intraperitoneally injected in the mice weekly. Tumors were measured at indicated time points. (B) Representative images of the dissected tumors were shown. A ruler was used to

demonstrate the size of the tumors. (C) Quantification of tumor weights at the end point. (D) Representative immunohistochemistry (IHC) stainings of USP35 and FUCA1 in the human CRC tissues. (E) Box plot showing the relative FUCA1 levels in USP35-low and USP35-high patients (n = 30). Median USP35 or FUCA1 expression was defined as the cut-off point. (F) The correlation of the expression of USP35 and FUCA1 in the human CRC tissues by IHC staining (n = 30). (G) The expression levels of USP35 and FUCA1 in the human CRC tissues and adjacent tissues were detected by western blotting (n = 8). The data were shown as the mean ± SD. *: $p < 0.05$, **: $p < 0.01$, ***: $p < 0.001$, [#]: $p < 0.05$, [##]: $p < 0.01$, [###]: $p < 0.001$ based on the Student's t-test.

Supplementary Files

This is a list of supplementary files associated with this preprint. Click to download.

- SupplementaryInformationFileforUSP35FUCA11013.docx